Engineering Structures 193 (2019) 91–99

Contents lists available at ScienceDirect

Engineering Structures

journal homepage: www.elsevier.com/locate/engstruct

Probabilistic machine learning approach to bridge fatigue failure analysis due to vehicular overloading

Wangchen Yan[a,b], Lu Deng[a], Feng Zhang[c], Tiange Li[b], Shaofan Li[b,*]

[a] Key Laboratory for Damage Diagnosis of Engineering Structures of Hunan Province, Hunan University, Changsha, Hunan 410082, China
[b] Department of Civil and Environmental Engineering, University of California, Berkeley, CA 94720, United States
[c] School of Mechanics, Civil Engineering and Architecture, Northwestern Polytechnical University, Xi'an, Shanxi 710129, China

ARTICLE INFO

Keywords:
Fatigue damage
Machine learning
Probabilistic analysis
Steel girder bridge
Vehicle overloading

ABSTRACT

With the rapid development of freight transportation, truck overloading becomes very common and severe, posing a great threat to the safety of bridges, and it can even result in bridge failure. Traditional approaches investigating the overloading-induced fatigue damage on bridges, such as finite element analysis (FEA) and reliability analysis, have proven to be computationally expensive and model dependent. In this study, the prediction of fatigue failure probability of bridges due to traffic overloading was investigated by using the feedforward neural network and the Monte Carlo method. Our results show that based on a finite set of training data for the bridge under consideration, the proposed machine-learning-based approach can assist in providing an instantaneous assessment of the fatigue failure probability with high accuracy.

1. Introduction

Steel girder bridges, which are the most common bridge type in the United States [1], are vulnerable to fatigue damage under cyclic vehicular loading. Due to the rapid development of freight transportation, truck overloading becomes very common and severe worldwide. Repetitive vehicular overloading could induce large number of stress cycles, which reduce the safety of bridges and can even lead to fatigue failure. According to the survey by Hobbacher et al. [2], overloading and fatigue have been the two leading causes of the damage of composite and steel bridges. It is therefore strongly necessary to investigate the fatigue damage of steel girder bridges under vehicular overloading conditions.

Numerous studies have been conducted on vehicle-induced fatigue damage on bridges based on deterministic analysis methods, such as numerical simulations, experiments, traffic surveys, and site tests. Cha et al. [3] estimated the effect of overloaded vehicles on the durability of steel girder bridges using the finite element (FE) model updating approach adjusted by field inspection data. Chen and Li [4] utilized the traffic investigation to evaluate the deterioration of a reinforced concrete bridge due to the vehicle-induced fatigue damage. Wang et al. [5] proposed a design method, which was based on the vehicle-bridge coupled system, for new bridges considering vehicular overloading induced fatigue damage. Deng and Yan [6] further proposed an overweight permit checking method for existing bridges based on numerical simulations.

It should be noted that the most important part of the aforementioned approaches is to obtain the equivalent stress under traffic loading. In the AASHTO approach [7], a truck model with deterministic configurations as developed based on a large number of traffic survey data was adopted to represent the real traffic. However, it was criticized that the deterministic parameters cannot reflect the large variability in the parameters of real traffic [8], especially under conditions with overloaded trucks which are not considered in the current AASHTO LRFD code [7]. Moreover, the fatigue failure is a result of the damage accumulation and greatly influenced by the uncertainties from both truck traffic and bridge parameters [9]. Hence, it is more appropriate to estimate the fatigue damage based on probabilistic approaches [8,10]. It should be noted that all the aforementioned methods are highly computationally demanding due to the vast number of repetitive simulations and therefore bring a significant challenge for efficient evaluation of fatigue damage.

Recently, machine-learning-based approaches have gained attention owing to the capability of reducing the computational effort required for fatigue assessment, and some achievements have been made. Based on the dataset with a large number of crack patterns of reinforced concrete slabs and the corresponding fatigue life, Fathalla et al. [11] have developed an artificial neural network (ANN) to link the fatigue life of RC bridge decks with the inspected surface cracks and attempted to make a quick and quantitative prediction for the fatigue life of bridge

* Corresponding author.
E-mail addresses: ywchener@berkeley.edu (W. Yan), denglu@hnu.edu.cn (L. Deng), xycwoc@berkeley.edu (T. Li), shaofan@berkeley.edu (S. Li).

https://doi.org/10.1016/j.engstruct.2019.05.028
Received 20 October 2018; Received in revised form 22 March 2019; Accepted 10 May 2019
Available online 15 May 2019

Nomenclature

3D	three-dimensional
A	fatigue constant
ANN	artificial neural network
AL	axle-load-based
COV	coefficient of variation
FD	fatigue damage
FD_{Δ}	critical fatigue damage in terms of fatigue resistance
$FD(t)$	fatigue damage caused by overloaded trucks after t years of service
FE	finite element
FEA	finite element analysis
GW	gross-weight-based
$g(X)$	fatigue failure function
m	slope of the S-N curve
MSE	mean squared error
n_k	number of cycles experienced corresponding to the kth stress range S_k
N_k	fatigue life in cycles corresponding to the kth stress range
Num	number of truck passage in one year
P_f	fatigue failure probability
r_{AL}	proportion of the AL-overloaded trucks in the traffic
r_{GW}	proportion of the GW-overloaded trucks in the traffic
S_i	stress range induced by the AL-overloaded trucks
S_j	stress range induced by the GW-overloaded trucks
S_k	kth stress range
t	service time in years
W_AL	gross weight of AL-overloaded truck
W_GW	gross weight of GW-overloaded truck
WIM	weigh-in-motion

deck slabs. Lu et al. [8] developed a probabilistic truck load model based on the weigh-in-motion (WIM) data and utilized the uniform design and support vector regression approach to substitute the time-consuming FE simulations in assessing the fatigue reliability of steel bridge decks under the loading of probabilistic truck model. Although bridge deck is more vulnerable to the repetitive traffic loading, the deterioration of deck slab does not necessarily threaten the bridge safety [12]. Utilizing the same machine learning approach by Lu et al. [8], Zhu and Zhang [13] further investigated the fatigue reliability of the critical welded joints of a coastal cable-stayed bridge under stochastic vehicle, wind, and wave loads. Despite considerable effort in the fatigue reliability using machine learning, there is still a lack of machine-learning-based approach to assess the fatigue failure reliability of steel girder bridges, especially under overloading conditions. Therefore, it is desirable to provide an efficient approach of conducting probabilistic fatigue analysis which can reduce the computational effort required by traditional fatigue assessment methods.

In the present study, the fatigue failure reliability of a typical composite steel girder bridge under vehicular overloading was investigated based on a machine learning algorithm. The deterministic simulations were first performed to obtain the bridge responses under overloading conditions. It is noted that the overloaded truck traffic was considered as a combination of the axle-load-based (AL) overloaded trucks and gross-weight-based (GW) overloaded trucks. Then, in order to substitute time-consuming FE simulations, a feedforward neural network was developed, trained, validated, and tested. Finally, the trained artificial neural network was combined with the Monte Carlo method to predict the fatigue failure probability of steel girder bridges under the traffic overloading.

2. Traffic overloading

Besides the gross weight, vehicle-induced damage is also closely related to the truck configuration, more specifically, the axle load. Therefore, in this study, two overloading conditions, namely, the AL-overloading and GW-overloading were considered. Two types of trucks, the three- and five-axle trucks, were adopted to consider such overloading conditions, respectively. This adoption was based on the fact that three-axle trucks are more likely to exceed the axle load limit while five-axle trucks are more likely to exceed the gross weight limit. The configurations of these two trucks are illustrated in Fig. 1. Specifically, the configuration of the three-axle truck is based on the AASHTO HS 20-44 fatigue design truck, which was developed from the dimensions of over 27,000 trucks collected from thirty sites all over the United States [14] while the configuration of the five-axle truck is based on the AASHTO type 3S2 truck, which was demonstrated to comprise nearly half of the heavy trucks [15]. As a result, these two types of trucks together are believed to be able to represent the actual overloaded truck traffic.

According to Hwang and Nowak [16], highway traffic consists of roughly 20% three-axle trucks and 80% five-axle trucks; therefore the basic overloaded truck traffic was considered to consist of 20% AL-overloaded trucks and 80% GW-overloaded trucks in this study. Moreover, in this study, it was assumed that the proportion of the AL-overloaded trucks (r_{AL}) follows a truncated lognormal distribution with a mean value of 0.2 and a coefficient of variation (COV) of 0.15. Considering the fact that r_{AL} always falls within the range between 0 and 1.0 under real traffic conditions, the corresponding lower and upper limits were therefore taken as 0 and 1.0, respectively. By adjusting the proportions of trucks that are overweight on gross and axle group, the actual traffic composition can be modified accordingly. Similar approaches were adopted by other researchers [17].

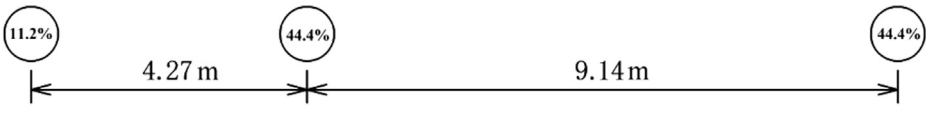

(a) AASHTO HS 20-44 fatigue truck

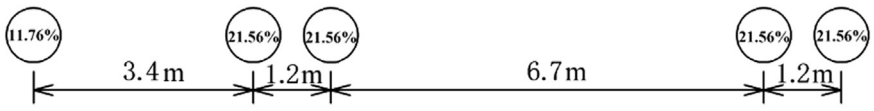

(b) AASHTO 3S2 type truck

Fig. 1. Truck models adopted.

In order to explore the effect of traffic overloading on the fatigue failure probability, the gross weights of the three- and five-axle trucks were both treated as random variables with normal distributions but with different mean values and COVs, as shown in Table 1. This assumption was adopted from [16]. Moreover, only the gross weights larger than that of the HS 20–44 and type 3S2 truck as specified in the AASHTO LRFD code [7], namely, 320 kN, were generated according to the corresponding distributions. According to the truck weight distribution based on the WIM data [18], the proportion of vehicles with gross weights over 512 kN is only 0.09%. Therefore, the effective gross weight for both the AL- and GW-overloaded trucks was set to be within the range from 320 kN to 534 kN. Moreover, the axle weight distributions of the AL- and GW-overloaded trucks are assumed to be the same as those of the AASHTO fatigue design truck and the type 3S2 truck, respectively, as illustrated in Fig. 1.

3. Framework of probabilistic analysis based on machine learning

3.1. Computational framework

In this study, with the attempt to substitute the time-consuming finite element analysis, the main work was conducted following three parts, as shown in Fig. 2.

In Part I, the input variables were selected and generated stochastically according to the corresponding distributions, and finite element analysis for the prototype of bridge under the overloaded truck traffic was performed to obtain the responses. Then, the rainflow counting method was utilized to calculate the cumulative fatigue damage. Finally, the limit state function of the fatigue damage accumulation was developed and its value was considered as the output.

In Part II, an artificial neural network was built based on the Matlab 2014a-Neural Network Toolbox. This neural network was then trained, validated, and tested based on the generated input and output data in Part I until satisfactory predictions were reached. In Part III, based on the trained ANN and the Monte Carlo method, the fatigue failure probability of bridge due to traffic overloading was predicted.

3.2. FE model of the prototype bridge

According to survey results, nearly half of bridges in the United States are composite steel girder bridges [1]. In this study, a typical composite steel girder bridge with a concrete deck slab was selected to illustrate the proposed framework. This bridge is a good representative of the simply-supported composite steel girder bridges with concrete deck slabs in the United States and has been widely used to investigate the fatigue performance of bridges [5,19]. In this study, a three-dimensional (3D) FE model of this bridge was developed with ANSYS software, as shown in Fig. 3. The bridge length is 30.48 m and the deck width is 9.75 m. It has five identical steel girders evenly arranged with an interval of 2.13 m in the transverse direction and five identical steel diaphragms spaced at a distance of 7.62 m in the longitudinal direction. The concrete bridge deck and the guardrail were all modeled by solid elements and the steel girders and diaphragms were modeled by shell elements. Similar schemes were adopted in many other studies to achieve a good balance between computational effort and desired accuracy [20–22]. The cross-section of the prototype bridge is shown in Fig. 4. More details of the bridge are listed in Table 2.

It should be noted that the bridge adopted in this study has two lanes, i.e., the fast lane and the slow lane as denoted by Lane 1 and Lane 2 in Fig. 4, respectively. According to statistics that over 90% of heavy trucks travel in the slow lane [8], and in this study only the scenario of overloaded trucks traveling in the slow lane was simulated, which is also suggested by the AASHTO LRFD code [7] for fatigue evaluation of bridges.

3.3. Probabilistic fatigue analysis

Under repetitive vehicular loadings, the number of stress cycles for the bridge undergone increases, causing the fatigue damage to accumulate accordingly. In this study, the limit state function for fatigue is defined in Eq. (1). The condition $g(X) < 0$ implies the fatigue failure of the bridge, and the probability of the event $g(X) < 0$ indicates the probability of fatigue failure.

$$g(X) = FD_{\Delta} - \sum_{i=1}^{t} FD(t) \tag{1}$$

where FD_{Δ} denotes the critical fatigue damage in terms of fatigue resistance; and $FD(t)$ is the fatigue damage caused by overloaded trucks after t years of service.

In order to explore the fatigue failure probability for the bridge under overloaded truck traffic, the influence factors (namely, the critical fatigue damage, the weight of overloaded trucks, the proportion of AL-overloaded trucks, and service time) were considered in this study. The critical fatigue damage (FD_{Δ}) was assumed to follow a truncated lognormal distribution with a mean value of 1.0 and a COV of 0.15 [23]. The critical fatigue damage generally ranges from 0.5 to 2.0 [4], which were selected as the lower and upper limits of FD_{Δ}, respectively. In addition, the fatigue damage accumulation was calculated based on the Miner's rule integrated with the S-N curve in this study, which is one of the most common approaches to calculate the fatigue damage, as shown in the following:

$$FD(t) = \sum_{k} \frac{n_k}{N_k} = \sum_{k} \frac{n_k \cdot S_k^m}{A} \tag{2}$$

where n_k and N_k denote the number of cycles experienced and the fatigue life in cycles corresponding to the kth stress range S_k, respectively; m denotes the slope of the S-N curve; and A denotes the fatigue constant.

It should be noted that in spite of some other fatigue-prone structural components, the condition of bridge girders generally controls the safety of girder bridges, and therefore the fatigue details of bridge girders are the main target in the fatigue design of girder bridges. Moreover, it has been demonstrated that the bending moment is more critical than the shear force for the cross section design of small-to-medium-span bridges. Therefore, the bending stress of the fatigue details at the girder mid-span generally governs the fatigue design of the type of girder bridges under consideration [24]. According to the AASHTO LRFD code [7], the corresponding fatigue details are the welds connecting the bottom flange and the web of the steel girders, which were selected in the present study and the values of m and A can be taken as 3 and 3.93×10^{12} MPa^3, respectively. In fact, this location has been selected as the representative fatigue detail for the fatigue study of this kind of bridges in many other studies [5,25,26].

Considering the overloaded truck traffic with different truck weights and different proportions of AL- and GW-overloaded trucks, the induced fatigue damage (FD) can be rewritten as follows:

$$FD(t) = Num \cdot t \cdot \left(r_{AL} \cdot \sum_{i}^{t} \frac{n_i \cdot S_i^m}{A} + r_{GW} \cdot \sum_{j}^{t} \frac{n_j \cdot S_j^m}{A} \right) \tag{3}$$

where t denotes the service time in years, and it is assumed to follow a uniform distribution starting from 1 to any specific year of interest, such as the 225th year in this study; Num denotes the number of truck

Table 1
Statistics of parameters for three- and five-axle trucks.

Truck type	Distribution type	Mean value (kN)	Standard deviation (kN)
Three-axle truck	Normal	178	37
Five-axle truck	Normal	290	76

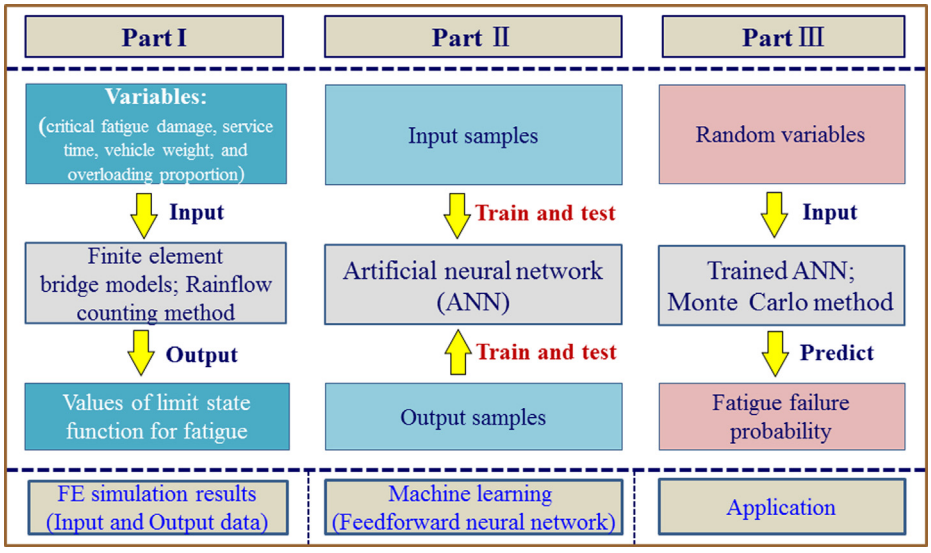

Fig. 2. Flow chart of the proposed framework based on machine learning.

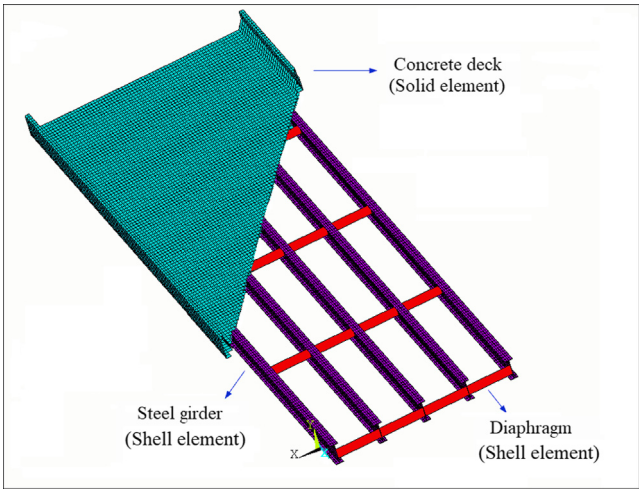

Fig. 3. 3D FE bridge model.

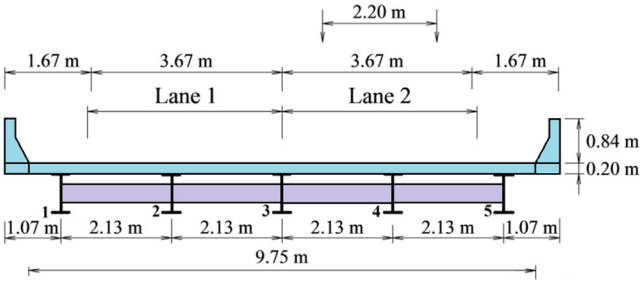

Fig. 4. Cross-section of the bridge under consideration.

passage in one year; r_{AL} and r_{GW} denote the proportions of the AL- and GW-overloaded trucks in the traffic, respectively; and S_i and S_j denote the stress range induced by the AL- and GW-overloaded trucks, respectively. In addition, the traffic growth is not considered and *Num* is calculated based on the average daily truck traffic (ADTT) suggested by the AASHTO LRFD code [7], namely, $Num = 365 \times 2000 = 730{,}000$.

Then the limit state function of the fatigue damage can be updated as follows:

$$g(X) = FD_{\Delta} - Num \cdot t \cdot \left(r_{AW} \cdot \sum_{i}^{t} \frac{n_i \cdot S_i^m}{A} + r_{GW} \cdot \sum_{j}^{t} \frac{n_j \cdot S_j^m}{A} \right) \quad (4)$$

Except for the distributions related to the gross weight of the AL- and GW-overloaded trucks listed in Table 1, the distributions for other variables selected in this study are summarized in Table 3.

The probability of the bridge fatigue failure due to traffic overloading during the service time, as defined in Eq. (5), is closely related to the reliability of the bridge [27]. According to Helmerich et al. [28], the target reliability index of existing bridges is generally in the range from 2.0 to 3.5 and the reliability of 2.0 corresponds to a failure probability of 2.3%. In this study, the target fatigue failure probability was selected as 2.3%, which was also adopted in other studies [8,13].

$$P_f = P(\ g(X) \quad \leqslant 0 \quad) \quad (5)$$

3.4. Probabilistic prediction of fatigue failure based on machine learning

A main objective of the technical approach is to efficiently fit the relationship between the output, namely, the value of $g(X)$, and the input variables, i.e., the gross weight of AL-overloaded trucks, gross weight of GW-overloaded trucks, proportion of AL-overloading, service time, and the critical fatigue damage. For this purpose, the feedforward neural network is adopted to learn the complex relationship between the input and output data. The feedforward neural network has proven to be capable of fitting any mapping problems [29], and it has been widely used in the civil engineering field due to its simplicity [30]. In this study, the feedforward neural network was built based on the platform of the Matlab R2014a-Neural Network Toolbox. The general structure of the feedforward neural network is shown in Fig. 5. In this study, the developed feedforward neural network has an input layer, an output layer, and eight hidden layers.

Table 2
Basic properties of the prototype bridge.

Roadway width	Concrete deck thickness	Girder height	Cross-sectional area	Moment of inertia	Young's modulus	Poisson's ratio
9.75 (m)	0.20 (m)	1.61 (m)	0.02 (m^2)	0.0011 (m^4)	210 (GPa)	0.25

Table 3
Distributions of the variables investigated.

Par.	Description	Distribution	Mean value	Standard deviation	Minimum	Maximum
FD_{Δ}	Critical fatigue damage	Truncated lognormal	1.0	0.15	0.5	2.0
r_{AL}	Proportion of AL-overloaded trucks	Truncated lognormal	0.2	0.15	0	1.0
N	Number of truck passage per year	Deterministic	2000			
t	Service time	Uniform			1	225
A	Fatigue constant	Deterministic	3.93×10^{12}	–		
m	Slope of S-N curve	Deterministic	3	–		

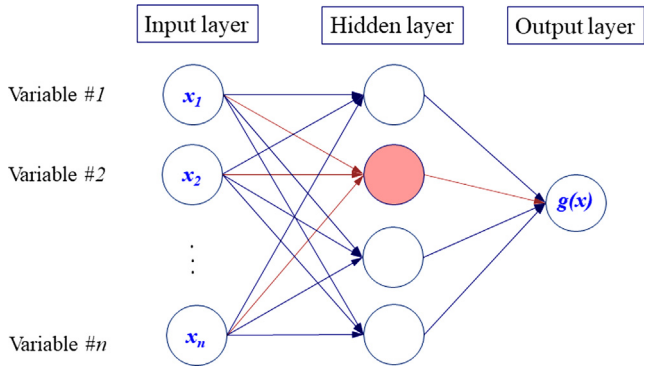

Fig. 5. Structure of the feedforward neural network.

In the feedforward neural network, data flow from the nodes in the input layer to the nodes in the hidden layers, and finally reach the nodes in the output layer. Each node in the hidden layers is a neuron which is the primary processing unit of the ANN. Generally, the neurons in the hidden layers have a summation block and an activation block to process the corresponding input data and transfer the output to the connected neurons in the next layer, as shown in Fig. 6. Taking the neurons in the $(l+1)$th hidden layer as an example, the tasks performed in the summation block and activation block are briefly outlined as follows:

1. **Summation block**: For the output neurons in the l-th hidden layer,

$$a^{(l)} = \begin{bmatrix} a_1^{(l)} \\ a_2^{(l)} \\ \cdots \\ a_n^{(l)} \end{bmatrix} \tag{6}$$

where l denotes the lth hidden layer; and n denotes the number of neurons in the lth hidden layer, and its stochastic weights were first assigned to each of them as follows:

$$W^{(l)} = \begin{bmatrix} W_{11}^{(l)} & W_{12}^{(l)} & \cdots & W_{1n}^{(l)} \\ W_{21}^{(l)} & W_{22}^{(l)} & \cdots & W_{1n}^{(l)} \\ \vdots & \vdots & & \vdots \\ W_{r1}^{(l)} & W_{r2}^{(l)} & \cdots & W_{rn}^{(l)} \end{bmatrix} \tag{7}$$

where $\boldsymbol{W}$ denotes the stochanistic weight; and r denotes the number of neurons in the $(l+1)$th hidden layer.

Then, the sum of all the weighted outputs was calculated to be the input to the ith neuron in the $(l+1)$th hidden layer as follows:

$$z_i^{(l+1)} = \sum_{j=1}^{n} W_{ij}^{(l)} a_j^{(l)} + b_i^{(l)} \tag{8}$$

where $z_i^{(l+1)}$ denotes the sum of the weighted inputs to the ith neuron in the $(l+1)$th hidden layer; and b denotes the bias to the ith neuron in the $(l+1)$th hidden layer.

2. **Activation block:** before entering the activation block, the bias terms were attached to neurons and added to the weighted sum. Then, the activation function was adopted to normalize the weighted sum, as shown in Eq. (8). In this study, the sigmoid function,

$$S(z) = \frac{1}{1+e^{-z}} \tag{9}$$

was adopted as the activation function to map the inputs of the neurons to values between 0 and 1. Adopting a non-linear activation function in this study allows the neural network to model the complex non-linear relationship. It is noted that the bias in Eq. (8) was used to shift the activation function.

In the artificial neural network, each neuron performs similar procedures shown in Fig. 6 and makes prediction eventually. After each cycle, the errors between the actual values and the predictions were calculated. Based on the calculated errors, the Levenberg-Marquardt optimization algorithm, which is a kind of gradient descent optimization methods and also the fastest backpropagation algorithm in the toolbox, was utilized to adjust the weights of neurons by calculating the gradient of the loss function. After repeating this procedure for a sufficiently large number of training cycles, the minimum gradient of the loss function could be reached and the training was then regarded as completed.

In this study, the mean squared error (MSE), defined as the average squared difference between the prediction and actual value, was selected as the index to examine the performance of the developed artificial neural network. The target value of MSE was set to be 0 which indicates a perfect prediction. During the training of the ANN, the MSE can be calculated at each epoch and the training stops until the MSE converges to a small enough value. The whole training procedure of the ANN is illustrated in Fig. 7.

Based on the generated input variables and the predicted outputs from the trained ANN, the Monte Carlo method was utilized to calculate the fatigue failure probability which is the ratio of the number of cases with $g(\mathrm{X}) < 0$ to the total number of samples investigated.

4. Results

4.1. Part I: Cumulative FD based on the FE analysis

In this part, a total of 150 sets of random input samples were

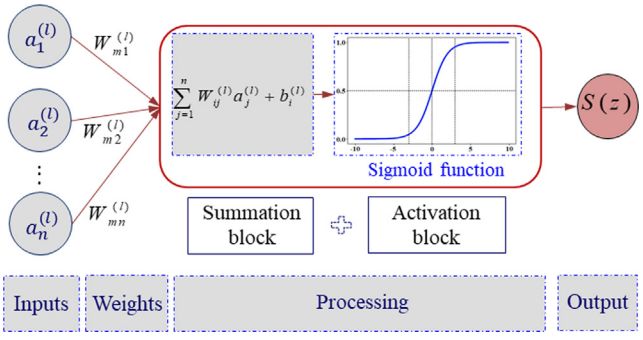

Fig. 6. Processing procedure of a single neuron.

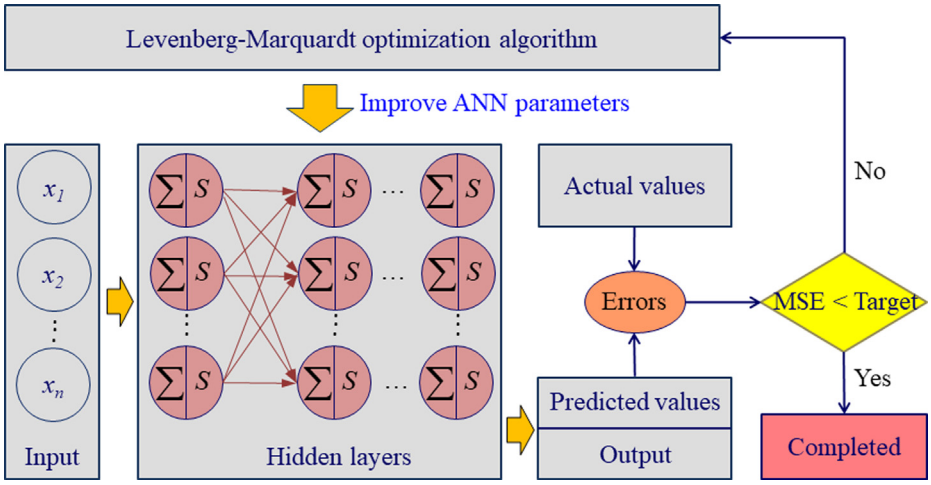

Fig. 7. Training procedure of the ANN.

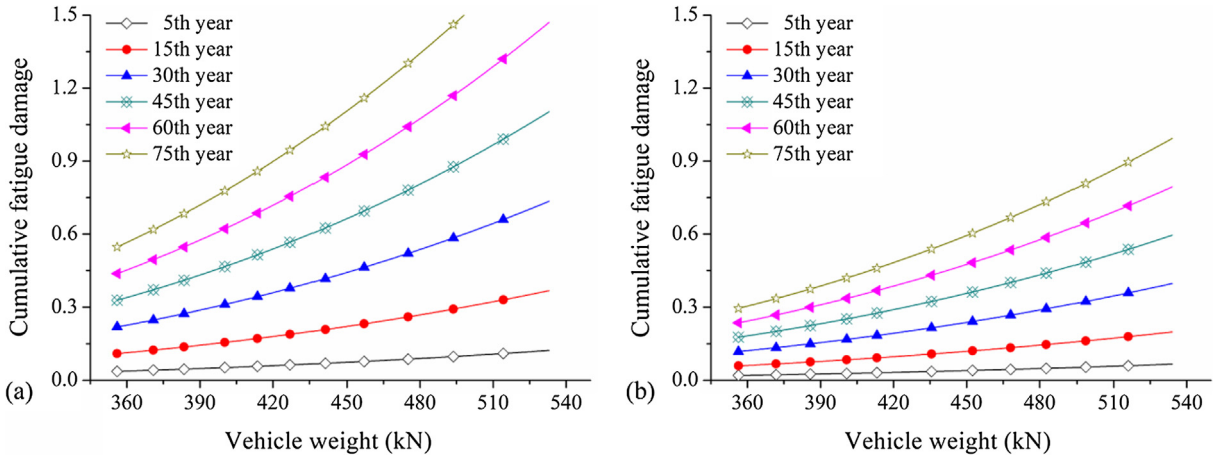

Fig. 8. Cumulative fatigue damage under overloading (a) AL-overloading; (b) GW-overloading.

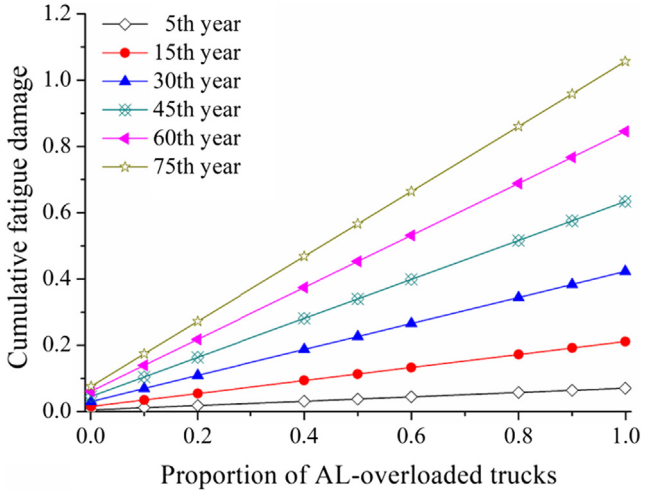

Fig. 9. Cumulative fatigue damage under overloading traffic with different proportions of AL-overload trucks.

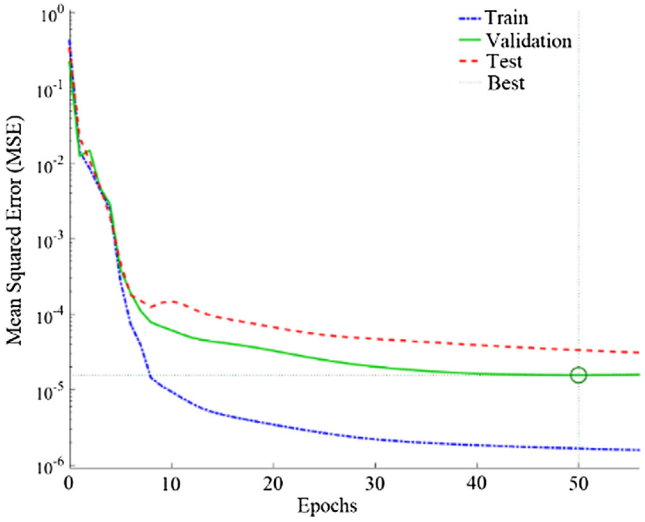

Fig. 10. Convergence of the MSE.

generated according to the corresponding distributions shown in Tables 1 and 3. For each set of the input samples, the finite element analysis was conducted to obtain the bridge responses under overloaded truck traffic, and the rainflow counting method was then utilized to calculate the induced cumulative fatigue damage. Assuming the overloaded truck traffic composed of AL-overloaded trucks only and GW-overloaded trucks only, the corresponding cumulative fatigue damage is shown in Fig. 8(a) and (b), respectively. It is evident that, under the same truck loading, the same time increment leads to nearly the same cumulative FD increment due to the linear fatigue damage accumulation adopted in

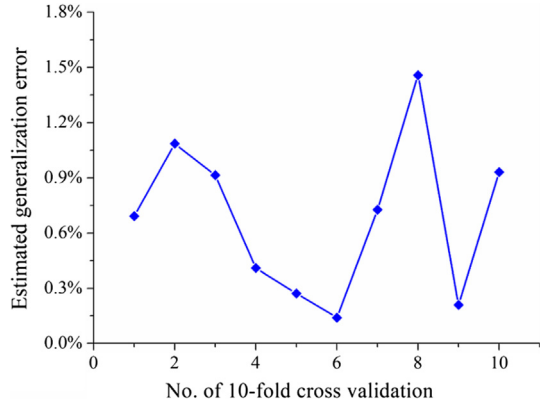

Fig. 11. Prediction errors of the best ANN.

Table 4
Difference between the ANN-based predictions and the FE results.

FD_Δ	t (year)	W_AL (kN)	W_GW (kN)	r_{AL}	g(X) based on FEA	g(X) based on ANN	Absolute difference
1.857	80	463.817	370.124	0.453	1.2468	1.2458	0.078%
1.172	15	444.700	499.295	0.294	1.0947	1.0943	0.032%
1.854	60	450.316	389.648	0.384	1.4887	1.4881	0.039%
1.805	45	442.794	485.294	0.102	1.6880	1.6884	0.027%
1.321	75	362.856	479.400	0.086	1.1864	1.1872	0.066%
0.838	30	436.658	477.166	0.660	0.5589	0.5585	0.083%
1.098	10	470.745	383.145	0.369	1.0314	1.0310	0.042%
0.700	50	515.621	448.541	0.011	0.6370	0.6360	0.160%
1.348	65	504.712	434.592	0.964	0.0411	0.0413	0.352%
0.747	15	528.248	530.867	0.366	0.6005	0.6003	0.020%

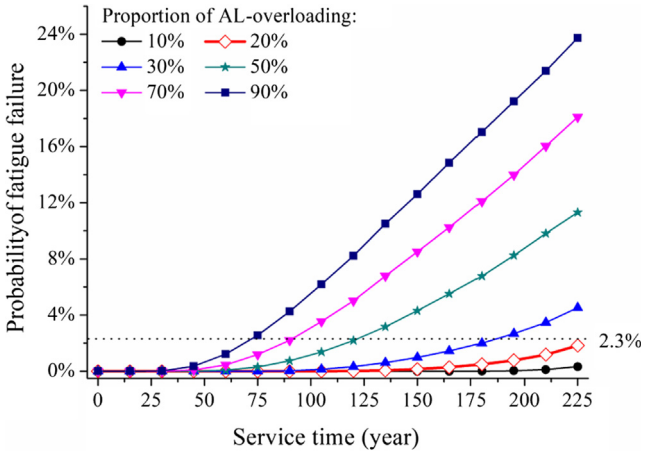

Fig. 12. Fatigue failure probability of the bridge under overloaded truck traffic.

this study, as shown in Eq. (2). However, as the vehicle weight increases, the difference between the adjacent cumulative FD with different vehicle weights also increases since the cumulative fatigue damage is proportional to the third power of the stress range (and therefore the vehicle weight).

The real truck traffic is usually composed of AL- and GW-overloaded trucks accounting for different proportions which can dramatically vary from site to site. In Part I, the cumulative FD under the overloaded truck traffic with typical proportions of AL-overloaded trucks, i.e., 0.1%, 10%, 20%, 40%, 50%, 60%, 80%, 90%, and 99.9%, is illustrated in Fig. 9. It should be noted that the sum of the proportions of the AL- and GW-overloaded trucks in the traffic is always equal to 1.0 in this study. It can be seen from Fig. 9 that the cumulative FD linearly increases as the proportion of AL-overloaded trucks grows. This phenomenon can be explained by the results in Fig. 8 that under the loading of truck with the same gross weight, both the cumulative FD and its increment caused by GW-overloading are obviously smaller than those caused by AL-overloading, which can be attributed to the more dispersed axle loads of five-axle trucks. In this regard, more attention should be paid to the axle load when determining the overweight limit.

Furthermore, as shown Fig. 9, the cumulative FD caused by overloaded truck traffic with different proportions of AL-overload trucks can be approximated by using the interpolation method, which is valuable for a quick estimation of the cumulative FD and the determination of overweight limit considering the vehicle-induced fatigue damage.

4.2. Part II: Train, validation and test of the ANN

In this study, the feedforward neural network was built to map the relationship between the output, namely, the value of the limit state function, and the input variables, i.e., the vehicle weight, proportion of AL-overloaded trucks, service time, and the critical fatigue damage. During the training procedure of the ANN model, as shown in Fig. 7, the mean squared error, which was used to measure the performance of the ANN, approaches to the target value of 0 as the number of epochs experienced increases. Fig. 10 illustrates the variation of the MSE for the optimized ANN. It should be noted that since the range of variation of MSE exceeded five orders of magnitudes during the whole process, a logarithmic scale for the MSE axle was utilized to capture the complete variation of MSE.

In order to improve the generality of the ANN model, the k-fold cross-validation method was adopted to assess the ANN model in this study. In the k-fold cross-validation method, the training data can be fully utilized, because all training data are used for both training and validation, which makes this method preferable for the case with small data samples.

In this study, the generated 150 sets of sample data were randomly divided into 10 equal sized subsamples, in other words, the 10-fold cross-validation method was adopted. For each training process, a single subsample was used as validation data and the remaining 9 subsamples were used as training data. And the process was repeated 10 times, i.e., each of the 10 subsamples was considered as validation data once. After the 10-fold cross validation process was completed, the average of the 10 predicted results was considered as a single estimation and the estimated generalization error can be calculated using Eq. (10).

$$CV_{(k)} = \frac{1}{k}\sum_{i=1}^{k} MSE_i \tag{10}$$

where $CV_{(k)}$ denotes the estimated generalization error under the k-fold cross-validation.

To achieve more accurate estimation, the 10-fold cross-validation was repeated 10 times and 10 generalization errors can be obtained, as shown in Fig. 11. The average value of the 10 generalization errors was then taken as the final prediction error. It should be noted that after the completion of each 10-fold cross-validation, the sample data were shuffled and split into 10 new equal sized subsamples to avoid duplication.

In this study, the optimized ANN model was chosen as the one producing the minimum estimation error. And the corresponding parameters of the optimized ANN model were all saved. Table 4 shows the g(X) under several typical conditions based on the FE analysis and prediction of optimized ANN. It is obvious that the maximum difference between the predictions and the FE results is only 0.352%, indicating the high accuracy of the ANN-based predictions.

4.3. Part III: Prediction of the fatigue failure probability

Based on the optimized neural network, the fatigue failure probability of the bridge due to overloaded truck traffic was investigated using the Monte Carlo method. Specifically, a total of 500,000 sets of input samples were generated stochastically according to the corresponding distributions listed in Tables 1 and 3. Then the corresponding 500,000 outputs were predicted simultaneously based on the optimized ANN model. Finally, the fatigue failure probability was calculated as the ratio of the number of negative outputs to the total number of outputs, i.e., 500,000.

Under the random gross weights of overloaded trucks considered in this study, several typical proportions of the AL-overloaded trucks, i.e., 10%, 20%, 30%, 50%, 70%, and 90%, and the service time from the 15th years to 225th years with an interval of 15 years were selected to illustrate the predicted fatigue failure probability, as shown in Fig. 12. It is necessary to mention that the target fatigue failure probability is selected as 2.3% in this study which corresponds to a target reliability index of 2.0 according to Helmerich et al. [28].

It can be seen from Fig. 12 that the fatigue life of the bridge under the loading of traffic with 20%, 30%, 50%, 70%, and 90% AL-overloaded trucks are 225, 188, 119, 89, and 74 years, respectively, with a fatigue failure probability of 2.3%. Furthermore, in the first 50 years, the difference among the fatigue failure probabilities under different proportions of AL-overloaded trucks is very slight and most of fatigue failure probabilities are slightly larger than 0. However, after 50 years of service, the difference becomes apparent. In addition, the higher the proportion of the AL-overloaded trucks, the higher the deterioration rate and the higher the fatigue failure probability. This clearly indicates the significant effect of AL-overloading on the fatigue life of bridges.

For the example used above, the total time spent in preparing the sample data and training the ANN is approximately 16 h based on a Core-7 computer, and only a few seconds are required by the optimized ANN to make predictions under a certain condition. Despite of the time spent in preparation, the efficiency of the proposed ANN-based probabilistic analysis method is reflected by its response time in damage evaluation in comparison with the traditional probabilistic fatigue methods. In specific, the proposed probabilistic machine learning has several distinct advantages: (1) the preparation of the training data is an one-time task for a specific bridge; (2) the trained ANN can make an accurate prediction for various scenarios within a few seconds for a fast decision-making process, while the traditional FE-based methods have to perform detailed FE analysis in order to complete a new task every time; (3) the probabilistic machine learning approach may have the potential to include the realistic measurement data in posterior fashion into the trained neural network, which will provide a great accuracy on the prediction of fatigue failure probability on top of time-response efficiency.

5. Concluding remarks

In this study, a probabilistic machine learning framework for predicting the fatigue failure probability of bridges under overloading is presented based on the ANN neural network and the Monte Carlo method. A typical composite steel girder bridge was used to illustrate the proposed framework. This approach is consisted of the following three steps: (1) collecting data based on finite element analysis; (2) training of the feedforward neural network; (3) predicting fatigue failure probability based on the optimized ANN.

Based on the deterministic analysis in this study, the cumulative fatigue damage under the overloaded truck traffic can be estimated using interpolation method, which is valuable for the traffic management and determination of overweight limit. Moreover, during the probabilistic analysis, it was found that the fatigue failure probability for the bridge does not increases linearly with time but increases more rapidly as service time increases. Therefore, more attention should be paid to bridges after years of service.

In this study, based on a finite set of training data, the feedforward neural network was trained to assist in providing an instantaneous assessment of the fatigue failure probability for a certain bridge. In addition, as a powerful artificial intelligence tool, machine learning can not only make predictions based on the regression of the existence of data, but also extrapolate unknown information through interpolation of the known events in the hyper-dimension event space. Therefore, the probabilistic machine learning approach may have the potential to include the realistic measurement data in posterior fashion into the trained neural network, which will provide a great accuracy on the prediction of fatigue failure probability on top of time-response efficiency.

Acknowledgements

The authors gratefully acknowledge the financial support provided by the National Natural Science Foundation of China (Grant No. 51778222 and 51478176), the China Scholarship Council (Grant 201706130087), and the Key Research Project of Hunan Province (Grant 2017SK2224).

References

[1] Bae HU, Oliva MG. Bridge analysis and evaluation of effects under overload vehicles (No. CFIRE 02–03). Nat Center Freight Infrastruct Res Ed (US) 2009.
[2] Hobbacher AF, Hicks SJ, Karpenko M, Thole F, Uy B. Transfer of Australasian bridge design to fatigue verification system of Eurocode 3. J Constr Steel Res 2016;122:532–42.
[3] Cha H, Liu B, Prakash A, Varma AH. Effect of local damage caused by overweight trucks on the durability of steel bridges. J Perform Constr 2014;30(1):04014183.
[4] Chen X, Li S. Fatigue damage assessment of the in-service bridge based on the traffic investigation. ICLEM: Log Sust Econ Dev: Infrastruct Inform, Integ 2010;2010:1537–43.
[5] Wang W, Deng L, Shao X. Fatigue design of steel bridges considering the effect of dynamic vehicle loading and overloaded trucks. J Bridge Eng 2016;21(9):04016048.
[6] Deng L, Yan W. Vehicle weight limits and overload permit checking considering the cumulative fatigue damage of bridges. J Bridge Eng 2018;23(7):04018045.
[7] American Association of State Highway and Transportation Officials (AASHTO). LRFD bridge design specifications. Washington, D.C.; 2017.
[8] Lu N, Noori M, Liu Y. Fatigue reliability assessment of welded steel bridge decks under stochastic truck loads via machine learning. J Bridge Eng 2017;22(1):04016105.
[9] Chen NZ, Wang G, Guedes Soares C. Palmgren-Miner's rule and fracture mechanics-based inspection planning. Eng Fract Mech 2011;78(18):3166–82.
[10] Carpinteri A, Spagnoli A, Vantadori S. A review of multiaxial fatigue criteria for random variable amplitude loads. Fatigue Fract Eng Mater Struct 2017;40(7):1007–36.
[11] Fathalla E, Tanaka Y, Maekawa K. Remaining fatigue life assessment of in-service road bridge decks based upon artificial neural networks. Eng Struct 2018;171:602–16.
[12] Kayser JR, Nowak AS. Reliability of corroded steel girder bridges. Struct Saf 1989;6(1):53–63.
[13] Zhu J, Zhang W. Probabilistic fatigue damage assessment of coastal slender bridges under coupled dynamic loads. Eng Struct 2018;166:274–85.
[14] Snyder RE, Likins GE, Moses F. Loading spectrum experienced by bridge structures in the United States Report No. FHWA/RD-85/012. Warrensville, Ohio: Bridge Weighing Systems Inc.; 1985.
[15] Mason Jr JM. Effect of oil field trucks on light pavements. J Transp Eng 1983;109(3):425–39.
[16] Hwang ES, Nowak AS. Simulation of dynamic load for bridges. J Struct Eng 1991;117(5):1413–34.
[17] Laman JA, Nowak AS. Fatigue-load models for girder bridges. J Struct Eng 1996;122(7):726–33.
[18] Schilling CG, Klippstein KH. Fatigue of steel beams by simulated bridge traffic. J Struct Div 1977;105(1):260–1.
[19] Wang TL, Liu C, Huang D, Shahawy M. Truck loading and fatigue damage analysis for girder bridges based on weigh-in-motion data. J Bridge Eng 2005;10(1):12–20.
[20] Mabsout ME, Tarhini KM, Frederick GR, Tayar C. Finite-element analysis of steel girder highway bridges. J Bridge Eng 1997;2(3):83–7.
[21] Baskar K, Shanmugam NE, Thevendran V. Finite-element analysis of steel–concrete composite plate girder. J Struct Eng 2002;128(9):1158–68.
[22] Eom J, Nowak AS. Live load distribution for steel girder bridges. J Bridge Eng 2001;6(6):489–97.
[23] Raju SK, Moses F, Schilling CG. Reliability calibration of fatigue evaluation and design procedures. J Struct Eng 1990;116(5):1356–69.
[24] González A, Cantero D, OBrien EJ. Dynamic increment for shear force due to heavy

vehicles crossing a highway bridge. Comput Struct 2011;89(23–24):2261–72.
[25] Deng L, Yan W, Nie L. A simple corrosion fatigue design method for bridges considering the coupled corrosion-overloading effect. Eng Struct 2019;178:309–17.
[26] Mori T, Lee HH, Kyung KS. Fatigue life estimation parameter for short and medium span steel highway girder bridges. Eng Struct 2007;29(10):2762–74.
[27] Melchers Robert E, Beck André T. Structural reliability analysis and prediction. West Sussex: John Wiley & Sons, Inc.; 2018.
[28] Helmerich R, Kühn B, Nussbaumer A. Assessment of existing steel structures. A guideline for estimation of the remaining fatigue life. Struct Infrastruct Eng 2007;3(3):245–55.
[29] Funahashi KI. On the approximate realization of continuous mappings by neural networks. Neural Networks 1989;2(3):183–92.
[30] Zhao J, Ivan JN, DeWolf JT. Structural damage detection using artificial neural networks. J Infrastruct Syst 1998;4(3):93–101.